8 Terrestrial propagation channel models

Chapter Editor: István Frigyes, BME, Budapest University of Technology and Economics.

Authors: László Csurgai-Horváth, BME, István Frigyes, Marlene Sabino Pontes, PUC, CETUC, Rio de Janeiro, Brazil, Irina Sirkova of Microwave Physics & Technologies Lab., Institute of Electronics, Bulgarian Academy of Sciences, Sofia, Bulgaria).

Content

8.1 Introduction

The application of wireless channels operating in microwave frequencies is one of the standard techniques in fixed communication systems since about the end of World War 2. During this period very detailed information on propagation characteristics of the microwave frequency band was gained and is available now. However, need for novel application arises continuously requiring in many cases more detailed knowledge on propagation. In this COST Action terrestrial systems were not of primary interest – thus number of contributions in this field was rather low.

Not-fully discovered domains and hot topics in which new results are needed and partly contained in this chapter relate to new frequency bands and propagation characteristics of particular geographical areas.

Among the new frequency bands what is called “60 GHz” is an about 7GHz band around 60 GHz, being particularly well suited to apply in very dense wireless networks both in cellular metropolitan networks and indoor. The interesting reason of this applicability is the extremely high attenuation caused by absorption spectral lines of Oxygen in this band and also the extremely high attenuation caused by walls and other indoor objects. Due to these short distance links can operate geographically close to each other without the risk of harmful interference. Also due to these characteristics 60 GHz is chosen to be licence-free band thus can be used free of charge. In the period of this COST Action no research was done in this field in Action-member institutes thus this Report does not contain any, more detailed description.

One of the, say, recent frequency bands belonging essentially to W-band (also called E-band) i.e. that of 71 to 76 GHz, 81 to 86 GHz and 92 to 95 GHz. Due to propagation characteristics this band is more suited to somewhat longer outdoor links and thus can form basis of metropolitan area backhaul networks. High reliability links can be realized of 1 or a few Gbit/sec capacity with hop-lengths – depending on climatological conditions – up to 2-5 km or so. Although this band is not free either from atmospheric absorption or from scintillation effects it is rain having the most harmful effect, that determines hop-length. In section 4 of this part of the Report BME results are described on E-band measurements and modelling.

Terahertz frequency band is one of particular interest and of hot topics in very different fields of technology, including (terrestrial) communication and communication in nanotecnologies. Although it is outside the explicit frequency limits of WG2, due to the increased interest a very short (and, of course, not exhaustive) review of fields of communication-related applications is given in section 5. Note that the Terahertz band can be regarded as a line of demarcation between *radio* and *optical* frequencies. A short discussion of this point is also given in section 5.

Among particular geographical regions it is the coastal and maritime propagation in which new results were achieved and are reported.

Going to details, one of the contributions, Section 2 (by Marlene Sabino Pontes) – presented here in full length – gives a rather detailed description of existing models with a long list of references (these dating from 1942 to 2008).

The next section (written by Irina Sirkova) presents modelling results on microwave propagation in coastal regions. First it discusses this problem as an example of the application and usefulness of the parabolic equation method in the solution of such complicated electromagnetic problems as this one. Next a method for statistical characterization of ducting is proposed via clustering of refractive index profiles.

Section 4 written by László Csurgai-Horváth (BME, Budapest University of Technology and Economics) presents results of BME-Budapest in three different fields. The first of these deals with Ku- and Ka-band second-order fade statistics, i.e. statistics of fade and interfade-duration. The second presents a new model for E-band (or other designation: W-band) rain attenuation; parametrers of ITU's rain attenuation models based on measurements made in Budapest are presented. And, the third deals with a BME-developed rain attenuation time series generator.

Section 5 contains a brief summary on THz applications and characteristics (written by the chapter editor, István Frigyes).

8.2 Review on terrestrial propagation channel modelling

Design and implementation of wireless systems, comprising mobile, portable and fixed radios, requires the knowledge of the propagation characteristics of the channel. The random nature of the radio channel and the complexity of the propagation phenomena suggest that the characterization of the channel can be achieved based on statistical analysis of field measurements. This approach leads to the statistical empirical models of the propagation channel. Alternatively, deterministic modeling, based on approximate solutions of the wave equation can be applicable in some situations.

For terrestrial systems, channel propagation modeling involves the prediction of the path loss, small and large-scale fading and depolarization effects. Measurements of path loss allow the probabilistic modeling of additional attenuation over free space loss [ITU-R P.525-2, 1994]. Additional attenuation is produced by propagation mechanisms such as atmospheric absorption, reflection, refraction, obstacle diffraction, multipath propagation effect, tropospheric scintillation and attenuation by foliage and by hydrometeors [ITU-R, 2008]. Multipath fading is the major outage causing mechanism on links longer than a few kilometers operating at frequencies below 10 GHz. On the other hand, precipitation attenuation dominates in microwave and millimeter bands above 10 GHz. The distribution of the received signal during rain depends on the climatic characteristics of the site or region where the link is located. In free space optical channels modeling, atmospheric absorption and scintillation must also be taken into account.

Large-scale fading in narrowband systems can be modeled from single frequency measurements. In clear-air conditions, the lognormal distribution usually describes the behavior of large-scale fading. Small-scale fading occurs mainly due to multipath effects and is characterized by deep and fast fluctuations on the signal envelope in a short period of time or distance. Minor displacements of the receiver modify the relationship between the phases of several components of signal generated by multipath. For mobile communications system, the receiver velocity also influences small-scale fading.

For narrowband channels, Rayleigh, Rice or m-Nakagami probability density functions can statistically describe the envelope of the received signal. Signals composed only by multiple path components have envelopes described by the Rayleigh distribution. Signals composed by multiple path components and a line-of-sight component are statistically described by Rice or m-Nakagami probability density functions [Parsons, 1992].

For wideband modeling, the channel impulse response can be represented as a sum of weighted delta functions, each component corresponding to a propagation path. The channel is usually described by the power delay profile and several related parameters as the RMS delay spread and mean delay spread in the time domain, and the Doppler spectra in the frequency domain [Parsons, 1992]. A channel exhibits frequency-selective

fading when the delay spread is greater than the symbol period. This condition occurs whenever the multipath components of a received symbol extend beyond the time duration of the symbols. When the delay spread is less than the symbol period, a channel is said to exhibit flat fading, and there is no channel-induced distortion. But there can still be performance degradation, due to irresolvable phasor components that add up destructively resulting in substantial reduction in signal-to-noise ratio at the receiver.

8.2.1 Clear Air Propagation Effects

8.2.1.1 Attenuation due to atmospheric gases

Absorption by oxygen and water vapor are always present and the resulting attenuation should be included in the calculation of total propagation loss at frequencies above 6 GHz. The calculation of the attenuation due to atmospheric gases on terrestrial and slant paths is given in ITU-R Recommendation [ITU-R P.676-8, 2009].n.

8.2.1.2 Diffraction loss

Diffraction loss depends on the type of terrain and the vegetation along the path. Methods for calculating diffraction loss for a single knife-edge obstruction, multiple obstacles, smooth spherical earth and also for paths with irregular terrain are discussed in ITU-R Recommendation [ITU-R P.526-11, 2009]. Recommendation ITU-R P.530-14 [ITU-R P.530-14, 2012] presents an approximation of diffraction loss over average terrain for losses greater than about 15 dB.

The classical solution of the diffraction over a smooth and homogeneous spherical Earth is given by the residue series [Bremmer, 1949]. Over, or beyond, the horizon the first term of this series provides a valid approximation for the evaluation of the diffracted field [Bullington, 1947; Rice et al., 1967].

The knife-edge model is an idealized model and relevant only in those cases where the radius of curvature of the obstacle can be neglected. An approximate equation [ITU-R P.526-11, 2009], originally derived by Boithias [Boithias, 1983], is given to evaluate the propagation loss relative to free-space due to a knife-edge, valid in the diffraction region. For the case of two knife-edges, rigorous solutions are available [Millington et al., 1962; Furutsu, 1963]. The theoretical solution for up to ten knife-edge obstacles requires the numerical evaluation of a multiple Fresnel-type integral of a dimension equal to the number of edges [Vogler, 1982]. For engineering purposes, approximate methods have been proposed [Epstein and Peterson, 1953; Deygout, 1966; Giovaneli, 1984], all based on the single-edge diffraction theory.

Hybrid methods and new models to consider the diffraction by irregular terrain integrating methods for smooth earth and irregular terrain have been published recently [Salamon and Wilson, 2008; DeMinco and McKenna, 2008; Willis et al., 2008; ITU-R, 2009a; ITU-R, 2009b].

8.2.1.3 Multipath propagation effects

Multipath results from different propagation mechanisms such as reflection and scattering caused by topography, buildings and obstacles, or by atmospheric refraction,

depending on the characteristics of the system and the environment. For terrestrial links fading due to multipath propagation is the most severe of various clear-air effects.

Two methods for predicting the single-frequency (or narrowband) fading distribution due to multipath in point-to-point links are given in ITU-R Recommendation [ITU-R P.530-14, 2012]. Both methods require the operation frequency, the path inclination, the altitude of the lower antenna, and a geoclimatic factor that depends on the behavior of the refractivity gradient in the region. One of those methods requires the knowledge of the path profile obtained from topographic data bases. ITU-R Recommendation [ITU-R P-530-14, 2012] also provides methods to obtain statistics of fade number and fade duration. This is relevant to predict availability and performance of line-of sight links. Unavailability is defined as the reception of signal below a chosen threshold (of received signal level for analog systems or bit error rate for a digital system) for more than 10 consecutive seconds or whenever the signal is totally interrupted. Events shorter than 10 seconds are considered to affect only the systems performance.

Due to the fact that multipath fading is frequency selective, the distortion induced at all amplitude levels in a wideband digital link can be a major outage source. Multipath induced distortion is likely to be the limiting factor for high capacity digital radio links for systems operating at frequencies below about 10 GHz. At higher frequencies the effects of the induced distortion must also be taken into account but, usually, the precipitation effects are much higher than the multipath effect.

For point-to-point systems, multipath propagation is usually described in terms of two or more discrete rays, given by amplitude and delay, and combined at the receiver. The number of rays may sometimes be large, but a deep fade occurs when two rays of comparable amplitude add destructively. It may well be that the deep fade (and frequency selective fading) is normally caused by one single ray arriving at a noticeable delay and adding to the other ray(s) that arrive earlier in time. To represent a limited bandwidth radio channel (40 - 100 MHz), simpler mathematical models may be used. These models may be classified as hypothetical or polynomial ray models. Hypothetical ray models are not physical because of the simplifications assumed in the expression of the transfer function. The simplified three rays model, also called the Rummler model [Rummler, 1978], is widely used by system planners. Alternatively, both real and complex polynomials can be used to represent the transfer function.

Orthogonal polarizations may be used independently for transmission at the same frequency channel over the same path to increase channel capacity without increasing bandwidth. However, this technique may be impaired by the possibility that, in propagation through the atmosphere, some of the energy transmitted in one polarization can be transferred to the orthogonal polarization, thus causing co-channel interference in frequency re-use systems. When signals in two orthogonal polarizations a and b are transmitted at the same level, the ratio of the co-polarized received signal (ac or bc) to the cross-polarized received signal (bx or ax) in that channel, is known as cross-polarization isolation (XPI) and frequently used in systems design. Propagation experiments, on the other hand, usually provide measurements of cross-polarization discrimination (XPD),

which is the ratio ac/ax when only the polarization a is transmitted. Although conceptually different, the XPI and the XPD may be considered to be the same for practical applications [23 Oguchi, 1973].

Due to the characteristics of the antenna patterns in both terminals, a cross polarized component will exist in the received signal even in normal propagation conditions through a standard atmosphere. The associated XPD can significantly deteriorate in clear air during periods of multipath propagation. ITU-R Recommendation ITU-R P-530-14, 2012] provides a method for estimation of XPD reduction in clear-air conditions that follows the approach developed in project COST 235 [COST 235, 1996] and relates XPD to the co-polar attenuation in the channel and parameters characterizing the cross-polar antennas patterns.

8.2.1.4 Coverage prediction models

For point to area systems operating in urban environments, narrowband channel modeling includes free space attenuation, diffraction caused by obstacles of the terrain, signal reflection, attenuation of rooftops and attenuation due to street crossings. In rural areas shadowing, scattering and absorption by trees and other vegetation can cause substantial path losses, particularly at higher frequencies [ITU-R P.833-6, 2007].

Semi-empirical models utilize approximate solutions to the multiple diffraction and reflection problems, where coefficients are adjusted with measured data taking into account all factors related to propagation. The use of empirical and semi-empirical models to predict propagation loss, although not so refined as ray-tracing techniques, takes a compromise between less accuracy and feasibility.

Existing prediction methods differ in their applicability over different terrain and environmental conditions. There is not a universal model that stands out as being ideally suited to all environments, so careful assessment is normally required. Most models aim to predict the median path loss, i.e, the loss not exceeded at 50% of locations and/or for 50% of the time. Knowledge of the signal statistics then allows estimation of the variability of the signal, so it is possible to determine the percentage of the specified area that has adequate signal strength and the likelihood of interference from a distant transmitter. Examples of propagation models for urban environments are the COST 231 Walfish-Ikegami, Ikegami, Walfish-Bertoni, Maciel and Xia models [Correia, 2001]. These models are combined to offer a mixed method [ITU-R P.1411-5, 2009] which can be used for both internal and external reception and it is applicable to transmitter configurations above or below rooftops. Its application is limited to micro and pico cells in an 1 km range from the transmitter. For distances beyond 1 km there is a set of methods for coverage prediction of macro cells, which considers free space attenuation and shadowing effects. Although these methods are less accurate than microcells models they require a smaller number of parameters for environment characterization. Examples of these models are Okumura-Hata [Okumura et al., 1968; Hata, 1980], COST 231 Hata [COST 231, 1991], SUI (Standard University Interim) [I.B.W.A.W.Group, 2003], and ITU-R Recommendation [ITU-R P.1546-4, 2009].

Okumura-Hata and COST 231 Hata are methods with analytical expressions adjusted to the graphical method of Okumura, which was developed from measurement campaigns in the 70s. The first is applicable to frequency range from 300MHz to 1500MHz, and the second one from 1500MHz to 2000 MHz. The SUI Model, based on the Erceg Model [Erceg, 1999], provides calculation of field strength for frequencies above 2000 MHz. It was basically derived from measurements in suburban areas, at distances extending to approximately 7 km.

The method [ITU-R P.1546-4, 2009] for point-to-area radio propagation predictions for terrestrial services is aplicable for frequencies in the range from 30 MHz to 3000 MHz. It is intended for use on links over land paths, sea paths and/or mixed land-sea paths between 1 to 1000 km length. The method is based on interpolation/extrapolation from empirically derived field-strength curves as functions of distance (1 to 1000 km), antenna height (10 to 1200 m), frequency (100 MHz, 600 MHz and 2000 MHz), percentage of local variability (1 to 99%) and percentage of time variability (1 to 50%). The calculation procedure includes corrections to the results obtained from this interpolation/extrapolation to account for terrain clearance and terminal clutter obstructions. The curves are based on measurement data mainly relating to mean climatic conditions in temperate climates as experienced in Europe and North America. Extensive studies reveal that propagation conditions in certain areas of super-refractivity bounded by hot seas are substantially different.

8.2.1.5 Time Variant and Wideband Channel Modeling

Characterization of wideband radio propagation channels can be developed from the general description of a linear time-variant channel. The behavior of the channel can then be described in terms of systems functions related to physical mechanisms which dominate the channel behavior.

Mathematical treatment of linear time-variant channels has started with Zadeh [Zadeh, 1950] with the introduction of the Time-Variant Transfer Function and the Bi-Frequency function as characterizing functions on the frequency domain. The author presented an analogy with transfer functions of fixed or non time-variant channels. This analysis technique in the frequency domain allowed the reduction of the complexity of the characterization techniques in time domain or the impulse response method in time domain. Kailath [Kailath, 1959] showed relationship between variables of the Time-Variant Transfer Function. In 1963 Bello [Bello, 1963] showed that filters or linear time-variant channels could be characterized in a symmetrical manner using variables in time domain or in frequency domain.

Concerning wideband channel characterization subject to influence of multipath, a seminal work has been done by Turin [Turin et al., 1972] and became the basis for other important works. Rummler's model, mentioned already in the previous section [Rummler, 1978] is essentially also dealing with multipath effect on wideband channels, i.e. with multipath-caused linear distortion. A widely used wide-band channel model is the one proposed by Saleh and Valenzuela [Saleh and Valenzuela, 1987] that describes the time-domain response of the channel considering multipath clusters. This model is

based on arrival time grouping of multipath components observed in experimental data. Extensive analysis of different wideband channel models is found in [Andersen et al., 1995; Mohammed et al., 2002]. More recently, the development of systems using multiple antennas techniques (MIMO) made necessary the development of spatial-time channel models [Ganesh and Pahlavan, 1991; Mohammed and Mahmoud, 1992].

In the case of mobile systems, the receiver has to be able to cope with the signal distortion arising from echoes in the channel as well as the rapid changes in the nature of this distortion. Such characteristics of the mobile radio channel are described by the power delay profiles and the Doppler spectra, which are obtained from wideband channel sounding measurements. The appropriate parameters for the statistical description of multipath effects can be computed either from instantaneous power delay profiles or from average power delay profiles. The latter are time averages obtained when the receiver is stationary that represent the movement in the environment or spatial averages obtained when the receiver is in motion [ITU-R P.1407-4, 2009].

8.2.2 Propagation Effects due to Rain

The physical mechanism of rain and the influence of rain events on radiowave propagation in terrestrial links over the troposphere are reviewed in this section. Focus is brought to the rain effects and on channel models that describe the statistical behavior of signal attenuation under rain conditions.

8.2.2.1 Precipitation characteristics

The size, shape and orientation distributions of raindrops may vary within a storm. Observations show that on average, the drop size distribution is relatively stable, changing mainly with rain rate. The Laws and Parsons drop size distribution [Laws and Parsons, 1943] has been found useful for the estimation of the attenuation and scattering properties of rain at frequencies up to 40 GHz. The relative densities of small drops having diameters less than 0.5 mm are not well modeled by the Laws and Parsons distribution and at frequencies above 40 GHz the Marshall-Palmer distribution [Marshall and Palmer, 1948] is used instead. The relative concentration of small drops can be highly variable and the use of a single model distribution may not be adequate for all locations.

Falling drops assume a nearly spheroidal shape when subject only to the effects of gravity and the surface tension of the water. The drops may vibrate and oscillate while falling but the net shape is oblate spheroidal with the symmetry axis close to vertical. Horizontal forces due to vertical wind gradients may cause the mean orientation to be canted by a few degrees. Pruppacher and Pitter [Pruppacher and Pitter, 1971] modeled drop shapes as a function of drop size. Observations in the laboratory by Pruppacher and Beard [Pruppacher and Beard, 1970] agreed with the shape predictions of Pruppacher and Pitter, but observations in the atmosphere tend to show smaller axial ratios than those calculated by the models for the same drop volume.

Gunn and Kinzer [Gunn and Kinzer, 1949] reported the terminal velocities of raindrops as a function of drop size. The velocities of the drops depend on air density and

are therefore a function of height. Radar observations show that on average the reflectivity value changes little with height below the rain height. The number and sizes of the drops and the liquid water content of a volume of drops therefore change little with height. As the specific attenuation depends primarily on liquid water content, the specific attenuation varies little with height below the rain height.

8.2.2.2 Cumulative distribution of point rainfall intensity

Measurements carried out with fast-response raingauges indicate that rainfall of high intensity tends to be concentrated in short periods of time, typically a few minutes. Consequently, experimental cumulative distributions of rainfall intensity depend on the integration time employed in the measurement. The monthly, daily and in some instances hourly rainfall accumulations readily available in the publications of various meteorological services cannot be utilized directly to obtain cumulative distributions of rainfall intensity down to small percentages of time. Models have been proposed to obtain distributions of rain intensity with 1 min integration time from the available distributions obtained with higher integration time [Capsoni and Luini, 2008; ITU-R P.837-5, 2007].

Rainfall of high intensity is difficult to record and measure experimentally, as well as being highly variable from year to year. In system design, however, it is the highest rainfall rates, which are frequently of great interest, and a suitable mathematical model for the "tail" of the distribution is desirable. At intermediate rainfall rates where accurate measurements are feasible, it appears that the cumulative rainfall rate distribution can be well approximated by a lognormal law. The range over which this relationship may be assumed valid depends somewhat on the climatic region, but typically it extends from 2 mm/h to about 50 mm/h. The gamma function has also been proposed as an approximation to the rainfall rate distribution [Morita and Higuti, 1976] although this function does not appear to be generally applicable in many climatic regions [Fefi, 1979]. Another analysis suggests that the rain rate distribution is better described by a lognormal distribution at low rates and a gamma distribution at high rain rate [Moupfouma, 1987].

Whenever appropriate rainfall intensity data exist for a certain location, these data should be used to determine the appropriate cumulative distribution. In the absence of such information the digital world maps of rain provided by ITU-R [ITU-R P.837-5, 2007] should be used.

8.2.2.3 Attenuation due to precipitation

Rain attenuation is the major propagation impairment for systems operating at frequencies above 10 GHz. The presence of hydrometeors, particularly rain, in the propagation path causes scattering and absorption of the propagating wave. The raindrops behave as dissipative dielectric media to the incident wave. The scattering is associated with modifications of wave propagation directions to satisfy boundary conditions at the raindrops surfaces. The absorption is due to dissipation, being a function of the drops conductivity. The combination of these two effects causes attenuation.

The specific attenuation γ_R (dB/km) at a given frequency may be obtained from the rainfall rate derived from the knowledge of the complex index of refraction of water at the temperature of the raindrops, the terminal velocity and the size distribution of the raindrops [Ryde and Ryde, 1945; Medhurst, 1965; Setzer, 1970]. Because of the non-spherical shape of the raindrops, horizontally polarized waves suffer greater attenuation than vertically polarized waves [Oguchi and Hosoya, 1974; Oguchi, 1977]. For practical applications the relationship between specific attenuation γ_R (dB/km) and rain rate R (mm/h) can be approximated by a power-law $\gamma_R = k\, R^{\alpha}$ [Olsen et al., 1978]. The recent work carried out by Gibbins and Walden [Gibbins and Walden, 2003] is the basis for ITU-R Recommendation [ITU-R P.838-3, 2005]. Values for the coefficients k and α are determined as functions of frequency, f (GHz), in the range from 1 to 1 000 GHz, which have been developed from curve-fitting to power-law coefficients derived from scattering calculations.

Attenuation due to rainfall along a path may be calculated by integrating the specific attenuation over the path length if the rainfall rate variation along the path is known. The field of rainfall rate is inhomogeneous in space and time [Callaghan and Vilar, 2003]. Rain gauge records show short intervals of higher rain rate imbedded in longer periods of lighter rain. Weather radar observations show small areas of higher rain rate imbedded in larger regions of lighter rain [Capsoni and D'Amico, 2004; Capsoni et al., 2006]. Such observations are typical of all occurrences of rain in all climate regions. Rainfall is often described as widespread or stratiform and as convective, but the differences between these types usually lie in the maximum rain rate to be associated with the rain process but not with differences in spatial variability.

The main difference in the various methods developed for predicting rain attenuation statistics from rainfall rate measurements is in the models used to describe the time-space structure of rainfall rate. The "synthetic storm method" generates attenuation statistics by converting rain rate/time profiles recorded at a point to rain rate/distance profiles, using the translation velocity of the rain pattern, this is estimated as the wind speed [Drufuca, 1974; Bertok et al., 1977; Segal, 1977; Kheirallah et al., 1980; Matricciani and Riva, 2008; Matricciani, 2008]. Recently there has been extensive work being carried out in time series synthesizers using the “synthetic storm technique” to provide rainfall time series [Lacoste et al., 2005].

All other methods make use of cumulative distributions of rainfall rate measured at a point. Some methods derive the statistical profile of rain along the path assuming a single cell of suitable shape [Misme and Fimbel, 1975], or a statistical distribution of sizes for cells of a particular shape [Capsoni et al., 1987a; 1987b; Paraboni et al., 2002]. Other methods characterize the statistical rain profile simply by a reduction coefficient which may be derived from the spatial correlation function of rainfall or from measurements using rapid response rain gauges spaced along a line [Harden et al., 1978; Crane, 1980], or from a semi-empirical law.

An alternative procedure is to apply the reduction coefficient to the actual path length, which yields an effective path length over which the rain intensity may be assumed to be constant [Lin, 1975; Garcia Lopez and Peiro, 1983; Moupfouma, 1984; Dissanayake and Allnutt, 1991]. This concept of an effective path length to take into account the non-uniform profile of rain intensity along a given path for the prediction of rain attenuation cumulative distribution on radio links is presently used in attenuation prediction methods such as those in ITU-R Recommendation ITU-R P-530-14, 2012]. System planning often requires the attenuation value exceeded for the time percentage of the "worst month". The conversion from annual statistics to "worst month" statistics is discussed in ITU-R Recommendation [ITU-R P.841-4, 2005].

Tests of the ITU-R rain attenuation prediction method against the measurements database currently available have shown that, on the average, the method significantly underpredicts the measured attenuations. A new or modified method proposed by China [ITU-R, 2005] is under consideration by the ITU-R.

ITU-R Recommendation [ITU-R P-530, 2012] also provides a method for the prediction of combined rain and wet snow. The method [Tjelta et al., 2005] makes use of a global map for the rain height and indirect information to make an estimate of the amount of wet snow and an average attenuation profile to obtain excess attenuation in the melting layer.

The procedures for determining the statistics of duration of rain induced fades can be found in ITU-R Recommendation [ITU-R P.530-14, 2012]. Although there is little information as yet on the overall distribution of fade duration, there are some data and an empirical model for specific statistics such as mean duration of a fade event and the number of such events. An observed difference between the average and median values of duration indicates, however, a skewness of the overall distribution of duration. Also, there is strong evidence that the duration of fading events in rain conditions is much longer than those during multipath conditions.

8.2.2.4 Depolarization due to precipitation

The shape of raindrops, as oblate spheroids, and the inclination to the horizontal are the two effects to cause cross-polarization during rain conditions. Most methods for prediction of XPD statistics during precipitation conditions now in use are semi-empirical [Saunders, 1971]. They are modeled on general theories for rain with randomly canted raindrops and with parameters chosen to give approximate agreement with experimental data. A two-parameter model based on a Gaussian distribution of raindrop canting angles is commonly assumed [Kobayashi, 1977; Nowland et al., 1977; Olsen, 1981]. For most practical applications, the relationship between cross-polarized discrimination (XPD) and the co-polarized path attenuation (CPA) is of the utmost importance for predictions based on attenuation statistics. ITU-R Recommendation [ITU-R P.530-14, 2012] provides a method to predict XPD from CPA and operation frequency.

8.2.3 Testing Propagation Prediction Models

Although deterministic models can be applied in some situations, the random nature of the radio channel and the complexity of the propagation phenomena suggest that, for engineering applications, most of the prediction methods currently in use are based on statistical empirical models derived from field measurements. This approach leads to statistical empirical models of the propagation channel. This section resumes the experimental data available and existing testing procedures for the modelling of propagation effects in terrestrial radio links.

8.2.3.1 Experimental data

The ITU-R databank - DBSG3 [ITU-R, 2011] was developed to collect experimental data existing in the technical literature and data submited by different parties. Data sets must comply with quality standarts that include experimental procedures for measurements and analysis, duration and uptime requirements. It is organized in 7 sections containing tables with experimental data related to:

I – Terrestrial line-of-sight path data (14 tables);

II – Earth-space path data (10 tables);

III – Terrestrial trans-horizon path & rain scatter data (4 tables);

IV – Radiometeorological data (10 tables);

V – Terrestrial land mobile data (2 tables);

VI – Terrestrial point-to-area data (1 table);

VII – Data for mobile-satellite services (4 tables).

Although the database structure is comprehensive, as to allow the modeling of propagation effects relevant to most communication systems operating in almost all frequency bands of interest, the amount of data available is limited. From the total of 44 tables, only 10 tables have a good amount of data (more than 50 datasets) to allow propagation modeling and 12 tables a fair amount of data to allow model testing. There are 15 tables with no data at all. The most critical sections are terrestrial land mobile data and terrestrial point-to-area data; perhaps currently the most important areas as far as current trends in communications systems are concerned. Table 1.3.1-1 details the existing tables and current status of DBSG3.

Besides the data collected during propagation measurement campaigns, there is a large amount of meteorological and Earth observation data, numerical weather forecast products, as well as meteorological data [ESTEC 18278, 2007] that provide information on basic parameters used in empirical and semi-empirical propagation models. Although mostly relevant to earth-space propagation models, some are also extremely relevant for terrestrial applications. The current trend to adopt digital maps of radio meteorological parameters, which are based on this database, in prediction methods represents a great advance in radio propagation modelling.

Table 8.2-1. Status of the terrestrial data tables in the ITU-R databank DBSG3

Table	Title	DBSG3 Status	Nr. Recs.
I	**Terrestrial line-of-sight path data**		
I-1	L-O-S rain attenuation statistics	C	63; 63; 26
I-2	L-O-S average worst-month multipath fading	C	286; 286; 0
I-3	L-O-S diversity data	C	38; 38; 0
I-4	L-O-S clear sky XPD and CPA statistics	C	16; 16; 0
I-5	L-O-S XPD and CPA statistics due to precipitation	C	11; 11; 0
I-6	L-O-S worst month multipath channel characteristics and outage times	C	82; 82; 0
I-7	L-O-S multi-hop worst month multipath fading and enhancement	C	0; 0; 0
I-8	L-O-S number of fade events and fade duration statistic	C	0; 0; 39
I-9	L-O-S annual attenuation statistics at optical wavelengths	N	0; 0; 0
I-10	L-O-S worst month attenuation statistics at optical wavelengths	N	0; 0; 0
I-11	L-O-S annual statistics of frequency diversity for millimetre and optical links	N	0; 0; 0
I-12	L-O-S worst mo. statistics of frequency diversity for millimetre and optical links	N	0; 0; 0
I-13	L-O-S time diversity statistics	N	0; 0; 0
III	**Terrestrial trans-horizon path & rain scatter data**		
III-1	Clear-air trans-horizon basic transmission loss statistics	C	202; 202; 12
III-1a	Clear-air spot measurement data	N	0;0; 0
III-2	Rain scatter on terrestrial paths	C	49; 49; 0
III-3	Joint signal level probability distributions	N	0; 0; 42

8.2.3.2 Model testing procedures

ITU-R Recommendation [ITU-R P.311-13, 2009] provides a general guidance on testing criteria for comparing propagation prediction methods that includes: (i) best performance, i.e., minimum mean of difference between predicted and measured value or minimum standard deviation of the difference; (ii) physical basis, specifically “the better the underlying physical principles are represented in a model, the better …” the method; (iii) simplicity as a third criterium, less relevant if its consideration is contradictory with the “physical basis requirement”.

The Recommendation also provides testing variables for rain attenuation, fade duration and fade slope predictions. For all other propagation effects and corresponding prediction methods, specific testing variables are yet to be defined.

Several limitations in the current testing procedures have been spotted, even for the cases in which specific testing variables are defined. There are several proposals under discussion for improving the current test variables. The two main concerns are: (i) the testing procedures should consider not only average error and its standard deviation but also outliers, i.e., particular cases in which extreme errors occur, particularly when these outliers are related to ranges of frequency, latitude, path lengths and other path characteristics; (ii) consideration of combined propagation effects relevant for specific

communication systems and instead of assessing the performance of individual prediction methods.

8.3 Microwave channel modelling in coastal and maritime areas

The propagation conditions in coastal and maritime regions are often complicated by the high variability of the meteorological parameters, local orography and sea surface state [Kerr, 1988]. Specific for coastal and maritime regions is one of the most challenging clear-air propagation mechanisms - the tropospheric ducting. The most common effect of ducting is the long-range radio waves propagation leading to signal enhancement near and beyond the radio horizon which provokes interference between terrestrial and Earth-space communications systems, [Milas and Constantinou, 2005]. Evaporation ducts, resulting of intensive evaporation from large bodies of water, are a major cause for multipath fading in over water links. This variety of influences requires the channel model in sea environment to account for simultaneous effects of diffraction, refraction, reflection and scattering propagation mechanisms. During the last two decades, the Parabolic Equation (PE) method [Levy, 2000] has become one of the most widely used operational methods when precise modeling of the influence of complex propagation environments is needed.

8.3.1 The parabolic equation method

The Parabolic Equation (PE) method is a deterministic, full-wave propagation prediction method. As a paraxial approximation to the wave equation, the PE is easily solved numerically through marching algorithms. It allows implementation of complex boundary conditions and inclusion of different antenna patterns. The PE method uses as input terrain database and information about the tropospheric refractivity, thus it accounts simultaneously and accurately for the above mentioned propagation mechanisms and provides solutions when rays based or normal-modes based techniques are unreliable or too resource consuming. As output the PE provides path loss (*PL*) or propagation factor (*PF*) in dB. Recently proposed in the literature [Fabbro et al., 2006] formulae which account for the shadowing effect due to sea surface roughness have been implemented within the split-step Fourier based numerical scheme [Barrios and Patterson, 2002] for the simplest forward-scatter narrow-angle two-dimensional scalar PE and applied for microwave propagation under evaporation duct conditions [Sirkova, 2011]. The shadowing is accounted for by introducing a phase and amplitude correction to the well known and widely used Ament's roughness reduction factor (RRF) [Ament, 1953]. Figure 8.3-1 shows the effect of corrected RRF on the *PL* for the case of ducting propagation and the following parameters: frequency F = 5 GHz, evaporation duct thickness z_d = 25 m, omni directional transmit antenna at height z_a = 5 m. In Figure 8.3-1a) *PL* is calculated for smooth sea; Figure 8.3-1b) refers to *PL* based on original Ament's RRF and Figure 8.3-1c) presents *PL* for corrected Ament's RRF; u_{10} is the wind speed at 10 meters above the sea surface.

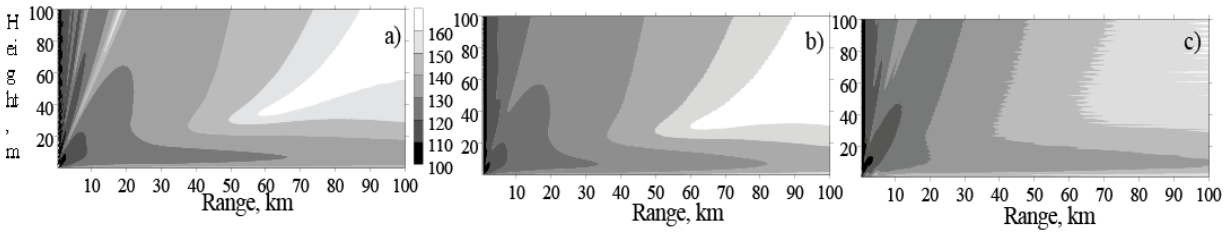

Figure 8.3-1: PL for evaporation duct conditions obtained for: a) smooth sea; b) original Ament RRF with u_{10}=10 m/s; c) corrected Ament RRF with u_{10}=10 m/s

The inclusion of the shadowing is expected to improve the propagation channel modeling and increase the coincidence between predicted and measured electromagnetic fields in the sea environment. The sea surface roughness destroys the duct structure and changes the *PL* pattern. The corrected Ament's RRF is more "destructive" than original Ament RRF especially as far the long-range ducted propagation is concerned. The higher frequencies are better guided by the duct but the increase of the frequency increases the importance of the shadowing and thus the long-range propagation of higher frequencies is impeded. The review paper [Sirkova, 2012] summarizes recent achievements and points out on some unresolved issues and ongoing developments related to further improvements of the PE method application to the propagation channel modeling in coastal and maritime areas.

8.3.2 Clustering of modified refractivity profiles

To take full advantage of a sophisticated propagation prediction method as the PE method, one should ensure adequate accuracy in the environmental modeling. For environments rich in ducting conditions, the accuracy in the reconstruction of the refractivity profiles serving as input to the propagation models determines in a great degree the fidelity of the acquired results. The standard approach to refractivity profiles restoration is based on some global [von Engeln and Teixeira, 2004] or local statistics [Mentes and Kaymaz, 2007] which provide the average duct parameters and occurrence but does not give characterization of the real form of the profiles. Another approach, assumed here, is to extract "characteristic" profiles for a given place and time (season) by examining modified refractivity *M* profiles computed from meteorological data for that place. The profiles are subdivided in groups (or clusters) depending on the specificities of their form. For each cluster a characteristic profile is extracted.

The meteorology is taken from the ECMWF current operational model, TL799L91, which uses 91 vertical levels with horizontal resolution of about 25 kilometers [Persson and Grazzini, 2007]. Data used refers to the Bulgarian shore of Black sea for two-year period (2007 and 2008) and encompasses four measurements per day (in 00 UTC, 06 UTC, 12 UTC, and 18 UTC). The specific location is some 10 to 60 kilometers far out to sea in the bay close to Varna (coordinates: 28^0E-43^0N; 28.5^0E-43^0N; 29^0E-43^0N). As the formation of trapping layers is concentrated in the first kilometer of the planetary

boundary layer, in this study the T_L799L91 levels from 91 (the closest to the earth surface) to 80 are used. It is to be noted that TL799L91 lowest level, 91, provides data at height of about 10 meters, i.e., evaporation ducts with thickness $z_d < 10$ meters are not included in the restored profiles. Thus, no differentiation between this type of duct and other surface ducts is made.

The global duct climatology [von Engeln and Teixeira, 2004] indicates the region of Black sea is characterized by high duct occurrence during summer time; basing on this as well as on old statistics, the month of July has been taken as representative for the summer season. The profiles for every of the three coordinates are examined separately this allowing to see the evolution of the profiles while going from the coast to the open sea. Even though a two-year statistics is too short to be representative and the height resolution of the T_L799L91 model does not allow catching the fine refractivity structure, it is enough to illustrate the idea of the refractive profiles clustering. Firstly, profiles very close to the standard one are excluded. For the remaining profiles, initially three clusters have been introduced: the first one contains profiles with elevated *M*-inversions, the second includes profiles with surface inversion, and the third takes in the profiles with some peculiarity that makes them differ from the standard profile. As a first step towards the determination of characteristic profiles, the median profile for each group (cluster) is generated. The preliminary results have indicated that a further differentiation between the profiles is to be done especially for cluster_I. This cluster encompasses profiles with elevated *M*-inversions responsible for the formation of different types of ducts: surface-based and elevated, thus, to be correctly represented, cluster_I needs additional subdivision. The difficulties with the introduction of metrics in order to refine the clusters come from the fact that it is not clear which trapping layer parameters (strength, thickness, height) are most important their importance being dependent on the frequency and the geometry of the problem as well. Nevertheless, after examining the profiles, the following two criteria for further subdivision of cluster_I have been chosen: first trapping layer bottom height and values of ΔM. The grouping of profiles with elevated layers has been formed around places of concentration of strong trapping layers. Depending of those criteria, cluster_I has been sub-divided in 3 groups with elevated layers: 1) first trapping layer bottom height between 240 and 320 m, $\Delta M \geq 13$, 2) first trapping layer bottom height above 420 m, $\Delta M \geq 13$, 3) other elevated layers with $\Delta M < 13$ (without regard of trapping layer bottom height) and one group for surface-based ducts formed by elevated inversions situated below 200 m. Once again, the median profile for every subcluster is generated.

On Figure 8.3-2 are shown the four proposed characteristic profiles for two of the coordinates. (For the third group of elevated layers ($\Delta M < 13$) no characteristic profile is extracted). Comparing the respective characteristic profiles from Figure 8.3-2 a) and b), it is seen that in the case of elevated inversions the characteristic profile (red line) reflects the increase in thickness of the higher elevated inversion (above 420 m) as going far out to the sea; in the case of surface-based duct (blue line) the characteristic profile catches the (possible) availability of a lower (due to evaporation) inversion for 29^0E-43^0N.

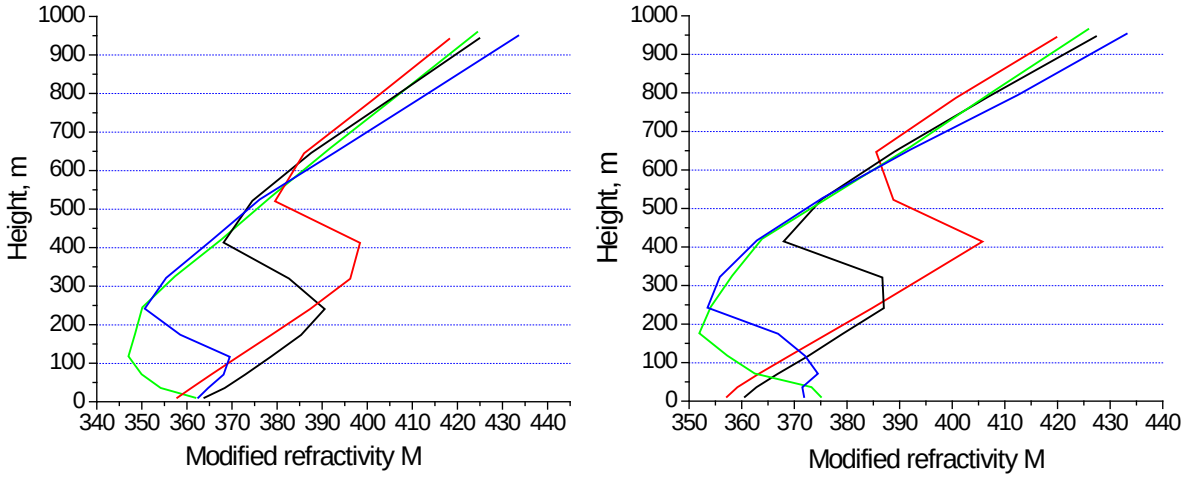

a) *b)*

Figure 8.3-2 The four proposed characteristic profiles for: a) 28^0E-43^0N and b) 29^0E-43^0N.

In this section an attempt is made to propose clustering of refractivity profiles with the aim to determine few (characteristic) profiles to be used as (typical for the given place) inputs to the electromagnetic models applied for further characterization of propagation channel. Note that the introduced metrics are site-specific and in dependence not only on the specificities of the refractivity profiles but also on the heights provided by the TL799L91 model. An availability of surface weather maps for the studied period would help to better interpret the statistics and make practical use of the proposed clustering. The study has demonstrated (once more) that in coastal and maritime environments the relying on the geographic proximity may be misleading; for those regions there is a strong need to account for the horizontal inhomogeneities of the refraction and to use range-dependent refractivity profiles.

8.4 Second order characterization, W(or E) band modelling and time-series generation: BME results in terrestrial channel modelling

8.4.1 Fade and interfade duration models for Ku-Ka band

Fade and interfade duration is one of the most important second-order statistics of the radio wave propagation. The lengths of the individual fade event, or the fading-free period duration provides very important knowledge for radio link planners in order to design for appropriate reliability and error-free operation. Several years of Ku-Ka band terrestrial radio link measurements helped the researchers at BME to develop digital models for such connections, which are applicable to calculate the fade and interfade duration statistics.

Our further investigations are proved that the attenuation process on terrestrial link is wide-sense stationary [L. Csurgai-Horváth and J. Bitó, 2007, b]. By introducing the concept of digital fade and interfade duration processes (DFD and DIFD) [L. Csurgai-Horváth and J. Bitó, 2008] we found that the DFD process is non-renewal, while the DIFD is renewal and both of them are low, mainly first order Markov processes. According to these results, the Fritchman's Markov model [L. Csurgai-Horváth and J. Bitó, 2009] has been selected to model the fade and interfade duration processes. This model can be parameterized from the fade and interfade duration statistics of the measured long-term attenuation time series. As fade and interfade duration is always defined as the function of threshold, the threshold dependency of the model has been also expressed, resulting a more general model.

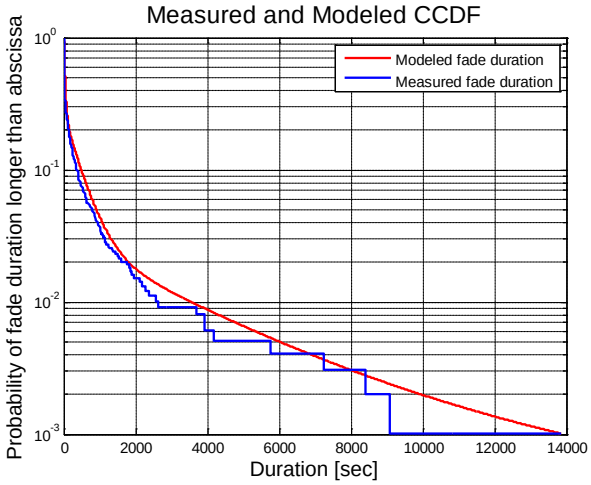

Figure 8.4-1. Measured and modelled fade duration distribution at 5 dB threshold

Our proposed models are easily applicable to generate synthetic attenuation time series, especially due to the arbitrary input parameter, the threshold.

8.4.2 Rain attenuation model for E-band

The development of wireless broadband terrestrial services are increasing the amount of transferred data, therefore the demand for new frequency bands, higher transmission speed or capacity is an actual problem. One of the possible solutions for this problem is the application of higher frequencies, for example the E-band. Besides the interference, the atmospheric and rain attenuation are possible the most important channel impairment factors of the E-band devices. At BME we have three years of measured data available for 72.56 GHz terrestrial radio link in urban environment; therefore attenuation and availability statistics could be investigated [I. Frigyes and L. Csurgai-Horváth, 2009]. According to the measurements we developed an empirical form to approximate the attenuation statistics in the E-band, furthermore some design considerations will be also introduced to build up short range -few kilometres length- of radio connections with specific availability requirements. In the next figure the measured attenuation CCDF is compared with the ITU-R proposed prediction [ITU-R Rec. P.530-12].

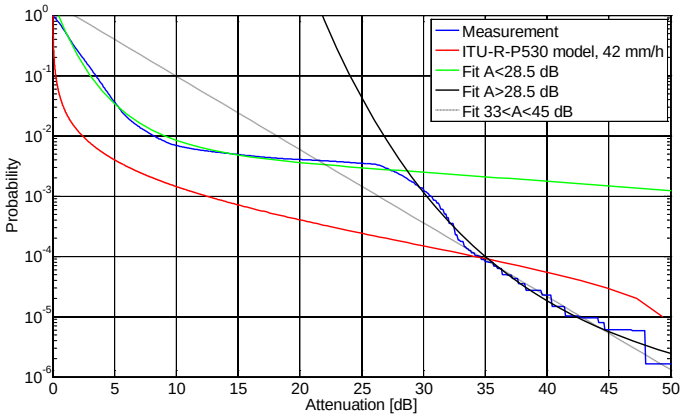

Fig. 8.4-2: New approximation of attenuation CCDF

For the E-band we propose an improved fit, by applying three different equations for the lower, higher and for the mid-range attenuations [L. Csurgai-Horváth, I. Frigyes, and J. Bitó, 2012].

8.4.3 BME rain attenuation time series generator

Attenuation time series generators may help to model the physical environment even if no real measurements are available at the investigated location. BME has been developed different rain attenuation time series generators for this purpose.

One of them is based on our fade and interfade duration models. In this model the fade events are generated with the threshold-dependent fade duration model, while the fading-free period length is estimated by using the interfade duration model [[L. Csurgai-Horváth and J. Bitó, 2007 a]]. A slightly modified approach is when the fade/non-fade sequences are generated with an appropriately parameterized two-state Markov chain, whose parameters are determined from the fade duration statistics. The fading periods are filled with synthetic fade events, generated by the fade duration model or with hidden

Markov-model [[L. Csurgai-Horváth and J. Bitó, 2007 b]. The fluctuation of the received signal, caused mainly by the atmospheric turbulences (scintillation), can be also synthesized and then superimpose on the attenuation time series [[L. Csurgai-Horváth and J. Bitó, 2007 a, c]. The method is also applicable to generate received power time series, if the frequency, polarization, path length, the transmit power and the antenna gains are known.

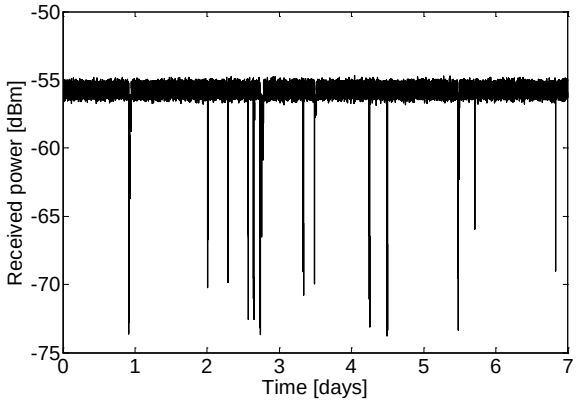

Fig. 8.4-3: Synthetic received power time series

A second method for attenuation time series generation is based on a stochastic model to simulate the movement of rain cells over the radio link area. Our solution is based on long term meteorological measurements. The statistics of wind speed and wind direction may lead to a combined Markov model to simulate the motion of a specific rain cell [J. Bitó & al.]. Furthermore, the size of the cell is determined by the local fade duration statistics, while the rain intensity in the rain cell centre follows the long-term rain intensity statistics. By running this combined model not only single rain events can be generated, but the long-term statistics of the synthetic time series are following the attenuation and even the second order statistics of the simulated radio links. A further advantage of this method is that the synthesized time series using this method can reproduce the small differences between physically closely arranged radio links, e.g. in star-structured topology.

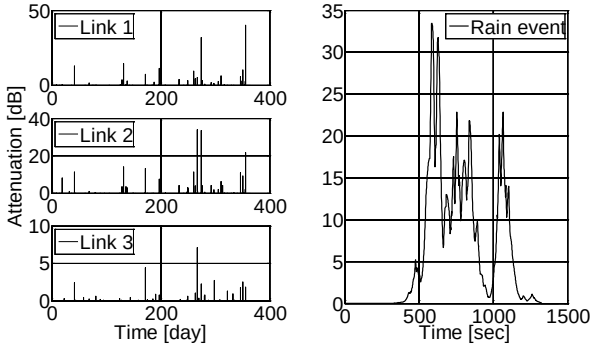

Fig. 8.4-4: Synthetic time series for star topology of radio links

8.5 A Brief Look on the Terahertz Channel

The mandate of the second Working Group of this Cost Action, according to the MoU contains radio frequencies up to W band (or: with recent designation E band) i.e. up to frequencies of 95…110 GHz. Thus what is called *Terahertz band* lies outside its scope; according to that during the years of the Action not too much interest was paid to this band. On the other hand, in recent years there was a vast interest in THz research and development, including investigations in propagation characteristics. Therefore it seems to be reasonable to give a very short glance on this technique, its application possibilities in communication and the main points in channel characteristics.

8.5.1 Terahertz waves: definition and possible fields of application

7 5 1 1 THz band - definition

As almost generally accepted definition states, the term Terahertz waves relates to the frequency band between 0,1 THz and 10 THz of electromagnetic fields, i.e. to wavelengths of 3 mm down to 30 μm. As already mentioned the interest increased very much about this band in recent years. An indication of that is: MTT-S (Microwave Theory and Techniques Society) of IEEE started recently (in November 2011) a new journal: *Transactions on Terahertz Science and Technology*.

The Terahertz band is at the boundary of the microwave/millimeter-wave and the infrared/optical band – to be characterized by very short wavelengths or by very small-energy photons. It is also at the boundary of two types of technologies, i.e. photonic and electronic technologies. That means that active components can be semiconductor devices resp. vacuum electronic devices on one hand with lasers or LEDs on the other hand; passive components/networks can be based on metallic waveguide structures vs. optical fibers and optical waveguides; as radiating elements antennas built of metallic structures (such as horn antennas) or of lenses and mirrors are equally applied or combination of these. Both approaches are valid and it depends on the special application which of them is more advantageous. A remark: being of this two-facedness, lines of demarcation are not uniquely defined. To see two examples of this situation: the fact that the Transactions cited above are published by the MTT-S shows that the microwave community feels that THz is an electric frequency range; at the same time: MoU of Cost Action IC1101 entitled “Optical Wireless Communication etc” states “Optical frequencies range from 300 GHz to 300 petahertz (PHz)”

In this IC0802 there was a short discussion about the THz domain. I.e. if occasionally it turns up: does it belong to WG2 or WG3 – the latter dealing with FSO (Free Space Optics). It was a (not very strong) feeling that WG2 is somewhat more appropriate.

8.5.1.2 Fields of application

Terahertz frequency band has many non-communication applications in biology, in chemistry in security-techniques, these mainly based on terahertz spectroscopy; these are

of course outside the scope of this report. There are three main fields of application being close to our topic, i.e. in astrophysics/radio-astronomy, in nanotechnology and in (more conventional) communications/sensing. (Of course, in nanotechnology it is also *communication* for which THz is used; however, *nano* use of it does not fit very well into the conventional communication concept.)

On the importance of the THz band in astrophysics see e.g. [Withington, 2003]. It is described that both the radiation peak of the microwave background radiation of the Universe and the emission spectral lines of colliding cold molecules are in this frequency band. Thus concrete knowledge on the formation of galaxies, planets or in general on cosmology is based on radio-astronomical observations in the THz band

In nanotechnology so called nano-machines perform the simplest operations; networks of nano-machines are able to increase both the complexity of taks and their range of operation. As discussed in [Jornet and Akyldiz, 2011] THz-band communication in graphene-based EM nanonetworks extend the possibilites of nano-technologies.

In (what we called here: conventional) communication the advantage of the THz band is the high frequency and the relevant high bandwidth. Consequently it is one of the possible bases of Gbit/sec wireless transmission (according to some estimations up to Tbit/sec (!)). Some of the publications in this topic are [Song and Nagatsuma, 2011], [Fitch and Osiander, 2004], [Piesiewicz & al., 2007], [Kleine-Ostmann and Nagatsuma, 2011]. Due to propagation characteristics very likely it is mainly short, indoor links which will operate in the THz band.

8.5.2 Propagation characteristics

Terahertz frequency band propagation is mainly influenced by atmospheric absorption. The main effect is that of water vapour. Water molecules have several absorption peaks (i.e. attenuation maxima) in this band, besides of a monotonic increase of attenuation vs. frequency. Between absorption peaks there are transmission windows; e.g. in the 0.1-3 THz band the number of major windows is 9 and the width of each of them is of the order of 100 GHz. Atmospheric absorption is discussed in a very detailed way (up to 1 THz) by [ITU P. 667-8, 2009].

In Fig.8.5-1 atmospheric attenuation – close to Earth surface – is shown in the 0.1…2 THz band is shown. Transmission windows can be seen, and also that attenuation minima are also rather high.

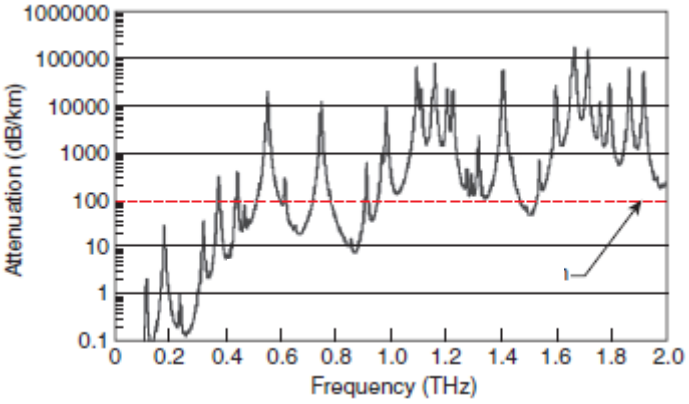

Fig. 8.5-1 Atmospheric attenuation vs. frequency

High atmospheric attenuation has its drawbacks but also some advantages. The main disadvantage is that it is not appropriate for application in long links. Thus the application is mainly confined to a few meters or, at most, to a few tens of meters; thus the main application (at least in the public domain) is for indoor links. As discussed, among others, in [Fitch and Osiander, 2004] and [Kleine-Ostmann and Nagatsuma, 2011] the need for Gbit/sec indoor links is existing already at present and will increase significantly by the end of this decade. In spite of the indoor application in outdoor links of about 100 m is not excluded. About fixed outdoor radio links see e.g. [Schneider & al. , 2012]

However, high attenuation can be an advantage in short links in military communication. This makes both interception and jamming rather difficult; further, the joint effect of narrow beams and high attenuation decreases to be corrupted by interference – either by friendly or by adversary users.

Length of indoor links makes atmospheric attenuation so to say irrelevant. However indoor usage may cause further problems. Objects in the room or hall cause reflection, diffraction and scattering; as a result of these multipath propagation and as a consequence increased loss and – due to the very wide band – linear distortion may occur. Also, as an effect of movement of persons in the room, originally LOS path may be shadowed or blocked. Several effects were investigated and published (e.g. [Priebe & al., 2011]) by the Technische Universität Brauschweig cited in this document.

Spending a few words on the effects of propagation phenomena on astrophysical use, of course large atmospheric attenuation constrains location of the relevant radio-telescopes to very special locations. These comprise the high plateau of the Antarctica (DATO), the Chilean Andes (CONDOR), Mauna Kea in Hawaii (more than 10 radio-telescopes) and a few others. And maybe: satellites are the most appropriate location to receive cosmic terahertz waves serving, of course, as relays for forwarding data via more appropriate frequencies to the Earth.

In nanotechnology applications the distances are very short, in the order of sub-millimetre. Thus loss is very low and so SNR and channel capacity can be very high

(capacity in the order of Tbit/sec). Concerning application in nanotechnology many papers are published by the Broadband Wireless Networking Lab. of Georgia Tech.

8.6 Conclusions

According to section 8.3 the method of Parabolic Equation (PA) is well suitable to solve special problems in coastal and maritime propagation. Clustering of characteristic refractivity profiles is proposed in order to ease electromagnetic modelling.

In section 8.4 three distinct topics are dealt with. 8.4.1 deals with second order statistics of the rain-induced-fade process. Main results – based on several years of Ku-Ka band terrestrial radio link measurements – are: the attenuation process is wide sense stationary; the digital model of interfade-duration represents a renewal process while that of fade duration not; both processes are in most cases first order Markov. In 8.4.2 a new model – valid for Budapest – is presented. And in 8.4.3 time series generators are described and validated

References

[Ament, 1953] Ament W.S. : “Toward a theory of reflection by a rough surface”, Proceedings IRE, Vol. 41, 1953, pp. 142–146.

[Andersen et al., 1995] Andersen J.B., Rappaport T.S., Yoshida S.: Propagation measurements and models for wireless communications channels”, IEEE Communications Magazine, vol. 33, pp.42–49, 1995.

[Barrios and Patterson, 2002] Barrios A.E., Patterson W.L. : “Advanced Propagation Model (APM). Computer Software Configuration Item (CSCI) Documents”, Spawar Systems Center San Diego Technical Digest 3145, 2002.

[Bello, 1963] Bello P.A.: ”Characterization of randomly time-variant linear channels", IEEE Trans. on Communications, v.11, pp. 360-93, May 1963.

[Bertok et al., 1977] Bertok E, Derenzis, G., Drufuca G.: “Estimate of attenuation due to rain at 11 GHz from rain gauge”, CNET, Issy-les-Moulineaux, France, pp. 295-300, 1977.

[Bitó & al 2008] J. Bitó, C. Capsoni, L. Csurgai-Horváth, L. Luini: “Modeling of Coherent Rain Cells Movement Affecting Terrestrial Radio Links”, 2nd JA2310 Workshop, München, Germany, 17/04/2008-18/04/2008. Paper 15.

[Boithias, 1983] Boithias L: Propagation des Ondes Radioélectriques dans l'Environnement Terrestre, Editions Dunod, Paris, 1983.

[Bremmer, 1949] Bremmer H.: “Terrestrial Radio Waves”, Elsiver Publishing Co., Amsterdam, The Netherlands, 1949.

[Bullington, 1947] Bullington K.: “Radio propagation at frequencies above 30 Mc/s”, Proc. of the IRE, vol. 35, no. 10, pp. 1122-1136, 1947.

[Callaghan and Vilar, 2003] Callaghan S.A., Vilar E.: “The spatial distribution of rain and its implications for wide area communications systems”, ICAP 2003, Exeter, 2003.

[Capsoni and D'Amico, 2004] Capsoni C., D'Amico M.: “Morphological description of the rain structures in the Padana Valley", Proceedings of the Third European Conference on Radar Meteorology (ERAD), pp. 541-544, Sweden, 2004.

[Capsoni and Luini, 2008] Capsoni C., Luini L.: “1-min rain rate statistics predictions from 1-hour rain rate statistics measurements”, IEEE Transactions on Antennas and Propagation, vol. 56, no. 3, pp. 815-824, 2008.

[Capsoni et al., 1987a] Capsoni C., Fedi F., Magistroni C., Paraboni A., Pawlina A.: “Data and theory for a new model of the horizontal structure of rain cells for propagation applications”, Radio Sci., vol. 22, no. 3, pp. 395-404, 1987.

[Capsoni et al., 1987b] Capsoni C., Fedi F., Paraboni A.: “A comprehensive meteorologically oriented methodology for the prediction of wave propagation parameters in telecommunication applications beyond 10 GHz", Radio Science, vol. 22, no. 3, pp. 387-393, 1987.

[Capsoni et al., 2006] Capsoni C., Luini L., Paraboni A., Riva C., “Stratiform and convective rain discrimination deduced from local P(R)", IEEE Transactions on Antennas and Propagation, vol. 54, no. 11, pp. 3566-3569, 2006.

[Correia, 2001] Correia L.M.: “Wireless Flexible Personalized Communications: COST 259: European Cooperation in Mobile Radio Research”, Wiley-Blackwell, 2001.

[COST 231, 1991] COST 231-Rev.2: “Urban transmission loss models for mobile radio in the 900 and 1800 MHz bands",1991.

[COST 235, 1996] COST 235: “Radiowave propagation effects on next-generation fixed-services terrestrial telecommunications systems, European Commission, EUR 16992 EN, ISBN 92-827-8023-6, 1996.

[Crane, 1980] Crane R.K.: “Prediction of attenuation by rain”, IEEE Trans. Commun., vol. 28, pp. 1717-1733, 1980.

[Csurgai-Horváth and Bitó, 2007, a] L. Csurgai-Horváth and J. Bitó: “Attenuation Time Series Generator with Markov Model of Fade and Interfade Durations”, Loughboroug Antennas and Propagation Conference, Loughborough, United Kingdom, 02/04/2007-03/04/2007. pp. 105-108.

[Csurgai-Horváth and Bitó, 2007, b]: Csurgai-Horváth, Bitó, “Rain attenuation time series synthesis with combined Markov models for microwave terrestrial links”, International Journal of Mobile Network Design and Innovation, Vol. 2. No. 3/4, pp. 216-222, 2007.

[Csurgai-Horváth and Bitó, 2007, c]: L. Csurgai-Horváth, J. Bitó, “Scintillation Time Series Synthesis for Satellite Links with Hidden Markov Model”, 2007 International Workshop on Satellite and Space Communications, Salzburg, Austria, 12/Sep/2007-14/Sep/2007, pp. 22-25.

[Csurgai-Horváth and Bitó, 2008]: L. Csurgai-Horváth and J. Bitó, “Renewal Properties of Rain Fade and Interfade Duration on Radio Links”, ICT Mobil Summit 2008, Stockholm, Sweden, 10/Jun/2008-12/Jun/2008, Paper 70.

[Csurgai-Horváth and Bitó, 2009]: L. Csurgai-Horváth and J. Bitó, 2009 “Testing the Markov Property of Rain Fading on Millimeter Band Terrestrial Radio Link”, EUCAP 2009, Berlin, Germany, 23/Mar/2009-27/Mar/2009. pp. 2901-2905.

[Csurgai-Horváth, Frigyes and Bitó, 2012] L. Csurgai-Horváth, I. Frigyes, J. Bitó, „Propagation and Availability on E-band Terrestrial Radio”, (accepted for EUCAP 2012)

[DeMinco and McKenna, 2008] DeMinco N., McKenna P.: “A comparative analysis of multiple knife-edge diffraction methods”, Proc. ISART/ClimDiff2008, paper ISART 10, pp. 65, 2008.

[Deygout, 1966] Deygout J.: “Multiple knife-edge diffraction of microwaves”, IEEE Trans. Ant. Prop., vol. 14, pp. 480-489, 1966.

[Dissanayake and Allnutt, 1991] Dissanayake A., Allnutt J.E.: “Interpretation of radiometric measurements of sky-noise in terms of path attenuation”, Proceedings ICAP 1991, pp. 374-378, 1991.

[Drufuca, 1974] Drufuca G., “Rain attnuation statistics for frequencies above 10 GHz from rain gauge observations”, Journal Recherches Atmospheriques, vol 1-2, pp. 399-411, 1974.

[Epstein and Peterson, 1953] Epstein J., Peterson D.W.: “An experimental study of wave propagation at 850 Mc/s”, Proc. of the IRE, vol. 41, No. 5, pp. 595-611, 1953.

[Erceg, 1999] Erceg V.: “An empririically based path loss model for wireless channels in suburban environments”, IEEE JSAC, vol.7, n.7, pp.1205-1211, 1999.

[ESTEC 18278, 2007] ESTEC 18278 Final Report: “Assessment of radiowave propagation for satellite communication and navigation systems in tropical and sub-topical areas”, 2007.

[Fabbro et al., 2006] Fabbro V., Bourlier C., Combes, P.F. : “Forward propagation modeling above Gaussian rough surfaces by the parabolic wave equation: introduction of the shadowing effect”, Progress in Electromagnetics Research, Vol. 58, 2006, pp. 243–269.

[Fedi, 1979] Fedi F.: “Attenuation due to rain on a terrestrial path”, Alta Frequenza, vol. XLVIII, 4, pp. 167-184, 1979.

[Fitch and Osiander, 2004] M. J. Fitch, R. Osiander, “Terahertz Waves for Communications and Sensing”, *Johns Hopkins Apl Technical Digest*, Vol. 25, Number 4 2004

[Frigyes and Csurgai-Horváth, 2009] I. Frigyes and L. Csurgai-Horváth „From Gigabit to Multi-Gigabit: mm Waves in Mobile Networks’ Backhaul”, IEEE Globecom 2009: International Workshop on Multi-Gigabit MM-Wave and Tera-Hz Wireless Systems (MTWS2009), Hawaii, United States of America, 30/11/2009-04/12/2009. pp. 8-13.

[Furutsu, 1963] Furutsu K.: “On the theory of radio wave propagation over inhomogeneous earth”, J. Res. NBS, vol. 67D, pp. 39-62, 1963.

[Ganesh and Pahlavan, 1991] Ganesh R., Pahlavan K.: “Statistical modeling and computer simulation of indoor radio channel”, IEE Proceedings Communications, Speech and Vision, vol. 138, pp. 153–161, 1991.

[Garcia Lopez and Peiro, 1983] Garcia Lopez J.A., Peiro J.: “Simple rain attenuation prediction technique for terrestrial radio links”, Elect. Letters, vol. 19, pp. 879-881, 1983.

[Gibbins and Walden, 2003] Gibbins C.J., Walden C.J.: “A study into the derivation of improved rain attenuation regression coefficients”, Radicommunications Agency Report No. AY4359, 2003, http://www.radio.gov.uk/topics/research/research-index.htm.

[Giovaneli, 1984] Giovaneli C.L.: “An analysis of simplified solutions for multiple knife-edge diffraction”, IEEE Trans. Ant. Prop., vol. 32, pp. 297-301, 1984.

[Gunn and Kinzer, 1949] Gunn R., Kinzer G.D.: “The terminal velocity of fall for water droplets in stagnant air”, J. Meteorol., vol. 6, n.4, pp. 243-248, 1949.

[Harden et al., 1978] Harden B.N., Norbury J., White A.: “Use of a lognormal distribution of raindrop sizes in millimetric radio attenuation studies”, IEE Conf. Publ. 169, part 2, pp. 87-91, 1978.

[Hata, 1980] Hata M.: “Empirical formula for propagation loss in land mobile radio services”, IEEE Transactions on Vehicular Technology, vol.29, pp.317-325, 1980.

[I.B.W.A.W.Group, 2003] I.B.W.A.W.Group: “Channel models for fixed wireless applications”, IEEE 802.16 Task Group Report, 2003.

[ITU-R P. 667-8, 2009] “Attenuation by Atmospheric Gases”, *ITU-R Recommendation* P.676-8, 2009.

[ITU-R P.1407-4, 2009] Recommendation ITU-R P.1407-4: “Multipath propagation and parametrization of its characteristics", 2009.

[ITU-R P.1411-5, 2009] Recommendation ITU-R P.1411-5: “Propagation data and prediction methods for the planning of short-range outdoor radiocommunication system and radio local area networks in the frequency range 300 MHz to 100 GHz, 2009.

[ITU-R P.1546-4, 2009] Recommendation ITU-R P.1546-4: “Method for point-to-area predictions for terrestrial services in the frequency range 30 MHz to 3000 MHz”, 2009.

[ITU-R P.1817, 2007] Recommendation ITU-R P.1817: “Propagation data required for the design of terrestrial free-space optical links”, 2007.

[ITU-R P.311-13, 2009] Recommendation ITU-R 311-13: “Acquisition, presentation and analysis of data in studies of tropospheric propagation”, 2009.

[ITU-R P.525-2, 1994] Recommendation ITU-R P.525-2: “Calculation of free space attenuation”, 1994.

[ITU-R P.526-11, 2009] Recommendation ITU-R P.526-11: “Propagation by diffraction”, 2009.

[ITU-R P.530-14, 2012] Recommendation ITU-R P.530-13: “Propagation data and prediction methods required for the design of terrestrial line-of-sight systems”, 2012.

[ITU-R P.676-8, 2009] Recommendation ITU-R P.676-8: “Attenuation by atmospheric gases", 2009.

[ITU-R P.833-6, 2007] Recommendation ITU-R P.833-6: “Attenuation in vegetation”, 2007.

[ITU-R P.837-5, 2007] Recommendation ITU-R P.837-5; “Characteristics of precipitation for propagation modelling", 2007.

[ITU-R P.838-3, 2005] Recommendation ITU-R P.838-3: “Specific attenuation model for rain for use in prediction methods”, 2005.

[ITU-R P.841-4, 2005] Recommendation ITU-R P.841-4: “Conversion of annual statistics to worst-month statistics”, 2005.

[ITU-R Rec. P.530-12] “Propagation data and prediction methods required for the design of terrestrial line-of-sight systems”, ITU, 2007.

[ITU-R, 2005] ITU-R Document 3M/107: “Proposed modification to Recommendation ITU-R P.530-10: An improved prediction method of rain attenuation for terrestrial light-of-sight path”, 2005.

[ITU-R, 2008] ITU-R Handbook, “Radiowave Propagation Information for Designing Terrestrial Point-to-Point Links”, 2008.

[ITU-R, 2009a] ITU-R Document 3J/64: “A New Approach to Diffraction Modelling for a General Path – The DELTA Method”, ITU-R SG3 WP 3J, 2009.

[ITU-R, 2009b] ITU-R Document 3J/100: “A Simple Corrected Deygout Multiple Knife-Edge Model – Application to general terrain diffraction prediction”, ITU-R SG3 WP 3J, 2009.

[ITU-R, 2011] ITU-R Databank: http://saruman.estec.esa.nl/dbsg3/login.jsp

[Jornet and Akyldiz, 2011], J.M. Jornet, I.F. Akyldiz, “Channel modeling and capacity analysis for electromagnetic wireless nanonetworks in the Terahertz band”, *IEEE Trans. on Wireless Comm.*, Vol 10, No. 10, pp. 3211-3221, Oct. 2011

[Kailath, 1959] Kailath T.: “Sampling models for linear time-variant filters, 1959.

[Kerr, 1988] Kerr D.E. (Ed.) : Propagation of short radio waves, Peninsula Publishing, Los Altos, 1988.

[Kheirallah et al., 1980] Kheirallah H.N., Segal B., Olsen R.L.: “Application of Synthetic Storm Data to Evaluate Simpler Techniques for Predicting Rain Attenuation Statistics”, Ann. Télécommunic, vol. 35, no. 11-12, pp. 456-462, 1980.

[Kleine-Ostmann and Nagatsuma, 2011], T. Kleine-Ostmann and T. Nagatsuma, “A review on terahertz communications research,” *J. Infrared, Millim. Terahertz Waves*, vol. 32, pp. 143–171, 2011.

[Kobayashi, 1977] Kobayashi T.: “Degradation of cross-polarization isolation due to rain”, Radio Research Laboratories Journal, vol. 24, pp. 101-107, July 1977.

[Lacoste et al., 2005] Lacoste F., Bousquet M., Castanet L., Cornet F., Lemorton J.: “Improvement of the ONERA-CNES rain attenuation time series synthesizer and validation of the dynamic characteristics of the generated fade events”, Space Communication Journal, Vol. 20, n°1-2, 2005.

[Laws and Parsons, 1943] Laws J.O., Parsons D.A.: “The relation of raindrop size to intensity”, Trans. Amer. Geophys. Union, vol. 24, pp. 452-460, 1943.

[Levy, 2000] Levy M. : Parabolic equation methods for electromagnetic wave propagation, IEE electromagnetic waves series 45, UK, 2000.

[Lin, 1975] Lin S.H.: “A method for calculating rain attenuation distributions on microwave paths”, Bell Syst. Tech. J., pp. 1051-1086, 1975.

[Marshall and Palmer, 1948] Marshall J.S., Palmer W.Mck.: “The distribution of raindrops with size”, J. Meteorol., vol. 5, 165-166, 1948.

[Matricciani and Riva, 2008] Matricciani E., Riva C.: “Test of the probability formulation of the Synthetic Storm Technique against reliable measurements of rain rate and rain attenuation“, Antennas and Propagation Symposium, 2008.

[Matricciani, 2008] Matricciani E.: “Global formulation of the Synthetic Storm Technique to calculate rain attenuation only from rain rate probability distributions“, Antennas and Propagation Symposium, 2008.

[Medhurst, 1965] Medhurst, R.: “Rainfall attenuation of centimeter waves: Comparison of theory and measurement”, IEEE Trans. Ant. Prop., pp. 550- 564, 1965.

[Mentes and Kaymaz, 2007] Mentes S.S., Kaymaz Z. : “Investigation of surface duct conditions over Istanbul, Turkey” Journal of Applied Metorology and Climaology, Vol. 46, March 2007, pp. 318-337.

[Milas and Constantinou, 2005] Milas V.F., Constantinou PH. : “Interference environment between high altitude platform networks (HAPN), geostationary (GEO)

satellite and wireless terrestrial systems", Wireless Personal Communications, Vol. 32, n°3-4, February 2005, pp. 257-274.

[Millington et al., 1962] Millington G., Hewitt R., Immiirzi F.S.: "Double knife-edge diffraction in field-strength prediction", Proc. IEE, vol.109C, pp. 419-429, 1962.

[Misme and Fimbel, 1975] Misme P., Fimbel J.: "Theoretical and experimental determination of rain-induced attenuation on a radioelectric path", Annales des Telecommunications, vol. 30, pp. 149-158, 1975.

[Mohammed and Mahmoud, 1992] Mohammed S.R., Mahmoud S.E.: "Space and frequency diversity measurements of the 1.7 GHz indoor radio channel using a four-branch receiver", IEEE Transactions on Vehicular Technology, vol. 41, pp. 312–320, 1992.

[Mohammed et al., 2002] Mohammed S., AL-Ahmadi, Shickh A.U.H.: "Spatial Domain Modeling Microcellular Systems Operating in Multipath Nakagami Channels", IEEE International Symposium on Personal Indoor and Mobile Radio Communications, 13, 2002, Dhahran – Saudi Arabia, vol. 4, pp. 1942- 1946, 2002.

[Morita and Higuti, 1976] Morita K., Higuti I.: "Prediction methods for rain attenuation distribution of micro and millimetre waves", Rev. Elec. Comm. Labs. NTT, vol. 24, pp. 7-8, 1976.

[Moupfouma, 1984] Moupfouma F.: "Improvement of a rain attenuation prediction method for terrestrial microwave links", IEEE Transactions on Antennas and Propagation, vol. 32, pp. 1368-1372, 1984.

[Moupfouma, 1987] Moupfouma, F.: "More about rainfall rates and their prediction for radio systems engineering", Proc. IEE. Part H, vol. 134, no. 6, pp. 527, 537, 1987.

[Nowland et al., 1977] Nowland W.L., Olsen R.L., Shakarofsky I.P.: "Theoretical relationship between rain depolarisation and attenuation", Electronics Letters, vol. 13, no. 22, pp. 676-678, October 1977.

[Oguchi and Hosoya, 1974] Oguchi T., Hosoya Y.: "Differential attenuation and differential phase shift of radio waves due to rain: Calculations of microwave and millimeter wave regions", J. Rech. Atmos., vol. 8, pp. 121-128, 1974.

[Oguchi, 1973] Oguchi T.: "Attenuation and phase rotation of radio-waves due to rain: Calculation of 19.3 and 34.8 GHz", Radio Science, vol. 8, pp. 51-58, 1973.

[Oguchi, 1977] Oguchi T.: "Scattering properties of Pruppacher-and-Pitter form raindrops and cross-polarization due to rain: calculations at 11,13, 19-3 and 34-8 GHz", Radio Sci.,12, pp. 41-51, 1977.

[Okumura et al., 1968] Okumura Y., Ohmori E., Kawano T., Fukuda T.: "Field strength and its variability in UHF and VHF land-mobile radio service", Rev. Elec. Commun. Lab., vol. 6, no. 9, 1968.

[Olsen et al., 1978] Olsen R., Rogers D., Hodge D.: "The aRb relation in the calculation of rain attenuation", IEEE Trans. Ant. Prop., vol. 26, no. 2, pp. 318- 329, 1978.

[Olsen, 1981] Olsen R.L.: "Cross polarization during precipitation on terrestrial links: A review", Radio Sci.. vol. 16. pp. 761-779, September and October 1981.

[Paraboni et al., 2002] Paraboni A., Masini G., Elia A.: “The Effect of Precipitation on Microwave LMDS Networks – Performance Analysis using a Physical Raincell Model”, IEEE J. on Selected Areas in Commun., vol. 20, no. 3, pp. 615-619, 2002.

[Parsons, 1992] Parsons J.D.: “The Mobile Radio Channel”, Halsted, New York, 1992.

[Persson and Grazzini, 2007] Persson A., Grazzini F. : “User Guide to ECMWF forecast products”, Version 4.0, March 2007, pp. 7-26.

[Piesiewicz & al., 2007] R. Piesiewicz, T. Kleine-Ostmann, N. Krumbholz, D. Mittleman, M. Koch, J. Schoebel, and T. Kurner, “Short-range ultra-broadband terahertz communications: Concepts and perspectives,” *IEEE Antennas Propag. Mag.*, vol. 49, no. 6, pp. 24–39, 2007

[Priebe & al., 2011] S. Priebe, C. Jastrow,M. Jacob, T.Kleine-Ostmann, T. Schrader, and T.Kürner, “Channel and propagation measurements at 300 GHz,” *IEEE Trans. Antennas Propag.*, vol. 59, no. 5, pp. 1688–1698, May 2011.

[Pruppacher and Beard, 1970] Pruppacher H.R., Beard K.V.: “A wind-tunnel investigation of the internal circulation and shape of water drops falling at terminal velocity in air”, Quart. J. Roy. Meteor. Soc., vol. 96, pp. 247-256, 1970.

[Pruppacher and Pitter, 1971] Pruppacher H.R., Pitter R.L.: “A semi-empirical determination of the shape of cloud and rain drops”, J. Atmos. Sci., vol. 28, pp. 86-94. January 1971.

[Rice et al., 1967] Rice P.L., Longley A.G., Norton K.A., Barsis A.P.: “Transmission loss predictions for tropospheric communications circuits”, NBS Tech. Note 101, vols. 1 and 2, U.S. Dep. of Commerce. (Available as AD687-820, Natl. Tech Inf. Serv., Springfield, Va.) [1965 (Rev. 1967)].

[Rummler, 1978] Rummler W.D.: “A multipath channel model for line-of-sight digital radio systems”, IEEE International Conference on Communications (ICC'78), Boston, USA, vol. 3, pp. 47.5.1-4, 1978.

[Ryde and Ryde, 1945] Ryde J.W., Ryde D.: “Attenuation of Centimetre and Millimetre Waves by Rain, Hail, Fog, and Clouds”, Rpt. No. 8670, Research Laboratory of the General Electric Company, Wembley, England, 1945.

[Salamon and Wilson, 2008] Salamon S., Wilson C.: “Reducing discontinuity in practical prediction of diffraction loss in irregular terrain”, Proc. ISART/ClimDiff2008, paper Diff.15, pp. 259, 2008.

[Saleh and Valenzuela, 1987] Saleh A.M., Valenzuela R.A.: “A statistical model for indoor multipath propagation”, IEEE Journal on Selected Areas of Communications, vol. 5, pp. 128-137, February 1987.

[Schneider & al., 2012] T. Schneider, A. Wiatrek, S. Preußler, M. Grigant, R. Braun, „Link budget Analysis…, IEEE Trans. Terahertz Science and Technology, Vol. 2, No 2, pp. 250-256, Feb. 2010

[Saunders, 1971] Saunders M.I.: “Cross polarisation at 18 and 30 GHz due to rain”, IEEE Trans., 1971, AP-19, pp. 273-277, 1971.

[Segal, 1977] Segal B.: Rain Attenuation Statistics for Terrestrial Microwave Links in Canada”, Commun. Res. Centre. Rep.No. 1351-E, Ottawa, Canada, pp. 14, 1977.

[Setzer, 1970] Setzer J.E.: “Computed transmission through rain at microwave and visual frequencies”, Bell System Tech. J., vol. 49, pp.1873-1892, 1970.

[Sirkova, 2011] Sirkova I. : “Propagation factor and path loss simulation results for two rough surface reflection coefficients applied to the microwave ducting propagation over the sea”, Progress in Electromagnetics Research M, Vol. 17, March 2011, pp. 151-166.

[Sirkova, 2012] Sirkova I. : “Brief review on PE method application to propagation channel modeling in sea environment”, Central European Journal of Engineering, Vol. 2, n°1, March 2012, pp. 19-38.

[Song and Nagatsuma, 2011] Song, H.J., T. Nagatsuma, “Present and Future of Terahertz Communications”, *IEEE Trans on THz Sci. and Techn.*, Vol. 1, No 1, pp. 256-263., Sept. 2011

[Tjelta et al., 2005] Tjelta T., Braten L.E., Bacon D.: “Predicting the attenuation distribution on line-of-sight radio links due to melting snow”, Proc. ClimDiff, Cleveland, U.S.A., 2005.

[Turin et al., 1972] Turin, G.L., Clapp, F.D., Johnston, T.L., Fine, S.B., Lavry, D.: “A statistical model of urban multipath propagation”, IEEE Transactions on Vehicular Technology, vol. 21, pp. 1–9, February 1972.

[Vogler, 1982] Vogler L.E: “An attenuation function for multiple knife-edge diffraction”, Radio Sci., vol. 17, No. 6, pp. 1541-1546, 1982.

[von Engeln and Teixeira, 2004] von Engeln A., Teixeira J. : “A ducting climatology derived from ECMWF global analysis fields”, Journal of Geophysical Research, Vol. 109, D18104, September 2004, doi:10.1029/2003JD004380.

[Willis et al., 2008] Willis M., Craig K, Thomas N.: “Measurement data for improving ITU-R Recommendation P.1812”, Proc. ISART/Climdiff 2008, pp.50-57, 2008.

[Withington, 2004] S. Withington, *Terahertz astronomical telescopes and instrumentation*, http://rsta.royalsocietypublishing.org/content/362/1815/395.full.pdf

[Zadeh, 1950] Zadeh L.A.: "Frequency analysis of variable networks", Proc.IRE,vol.38, pp.291-299, 1950.